Gamma-ray spectroscopy in ^{31}P: levels below 7.5 MeV (populated in ^{28}Si(α,pγ) reaction)

1974 J. Phys. A: Math. Nucl. Gen. 7 1410

(http://iopscience.iop.org/0301-0015/7/12/005)

J. Phys. A: Math., Nucl. Gen., Vol. 7, No. 12, 1974. Printed in Great Britain.

Gamma-ray spectroscopy in ^{31}P: levels below 7·5 MeV

P J Twin, E M Jayasinghe, G D Jones, P R G Lornie, A Nagel, H G Price and M F Thomas

Oliver Lodge Laboratory, University of Liverpool, PO Box 147, Liverpool L69 3BX, UK

Received 20 February 1974

Abstract. Gamma-ray angular distributions have been measured following the ^{28}Si(α, pγ)^{31}P reaction using both NaI(Tl) crystals, in coincidence with an annular particle telescope, and GeLi detectors. Lifetimes have been determined using the DSAM and γ-ray polarizations measured using a 3 GeLi Compton polarimeter. New definite spin assignments include $\frac{5}{2}^+$ (5115 keV state), $\frac{7}{2}^+$ (4634 and 6048 keV states), $\frac{9}{2}^+$ (5343, 5892, 6081 and 7118 keV states), $\frac{11}{2}^+$ (6453 and 7441 keV states), $\frac{3}{2}^-$ (5010 keV state), $\frac{9}{2}^-$ (6500 and 6793 keV states) and $\frac{11}{2}^-$ (6825 keV state). Many multipole mixing ratios, lifetimes and new branching ratios are reported.

An interpretation of the positive parity states is proposed based on the strong coupling and rotation–vibration models. A striking feature in the spectrum of the negative parity states is pointed out which suggests particle–phonon coupling is important. Shell-model calculations based on the MSDI interaction have been extended to include the transition strengths from higher spin positive parity states.

1. Introduction

The spins and parities of low-lying low spin states in ^{31}P have previously been extensively investigated using the ^{30}Si(p, γ)^{31}P reaction. These results have been summarized by Endt and Van der Leun (1973) including work using GeLi detectors reported by Wolff *et al* (1968) and Willmes and Harris (1967). Using the same reaction Wolff *et al* (1969) measured the lifetimes of states up to 5 MeV excitation energy, and l values and spectroscopic factors have been reported from an investigation of the reaction ^{30}Si(τ, d)^{31}P (Wolff and Leighton 1970). These experiments resulted in spin assignments for all states up to 5 MeV excitation energy (except that at 4634 keV $(\frac{5}{2}, \frac{7}{2})^+$), and the determination of branching ratios and several multipole mixing ratios. Comparisons were made with shell-model calculations using the surface delta interaction by Glaudemans *et al* (1969) and with intermediate coupling calculations by Castel *et al* (1970). The agreement with both models was quite good but experimental data were available only on low spin states with $J^\pi \leqslant \frac{7}{2}^+$.

The energies of 49 states below 8 MeV excitation energy have been reported by Moss (1969) using the ^{29}Si(τ, p)^{31}P and ^{30}Si(τ, d)^{31}P reactions. The majority of these states have also been observed in (p, γ) work and there is no evidence to suggest that the other states, mostly above 7 MeV, are high spin states. However, De Voigt *et al* (1971) in an investigation of the ^{27}Al(α, γ)^{31}P reaction propose new states of probable high spin at 6·08, 6·45, 6·50, 6·79, 6·83, 7·12 and 7·44 MeV, and report lifetime measurements on some of these states. However, due to the small reaction cross section, they were unable to carry out angular distribution experiments.

The present paper reports an extensive study of high spin states in ^{31}P using the $^{28}Si(\alpha, p\gamma)^{31}P$ reaction. The experimental techniques used are described in § 2, the results and conclusions for individual levels are reported in § 3, and possible interpretations of the states are given in § 4.

2. Experimental methods

2.1. Doppler shift attenuation method (DSAM)

The reaction $^{28}Si(\alpha, p\gamma)^{31}P$ was used to populate states in ^{31}P at alpha bombarding energies of 6·75, 8·5, 10·5, 12·0 and 14·0 MeV. The targets were 1 mg cm^{-2} ^{28}Si evaporated on to thick gold backings with an isotopic enrichment greater than 99·6%. The γ rays were detected in a GeLi–NaI(Tl) escape-suppressed spectrometer (Sharpey-Schafer *et al* 1971) and a spectrum taken at 10·5 MeV is shown in figure 1. The detector system was calibrated for energy and efficiency using γ rays from a ^{56}Co source, the energies and intensities being taken from the work of Scott and van Patter (1969).

Centroid positions of γ-ray lines were measured at angles of 0°, 30°, 45°, 60°, 70°, 90° and 110° and the attenuation factors F were obtained by linear least-squares fits to the

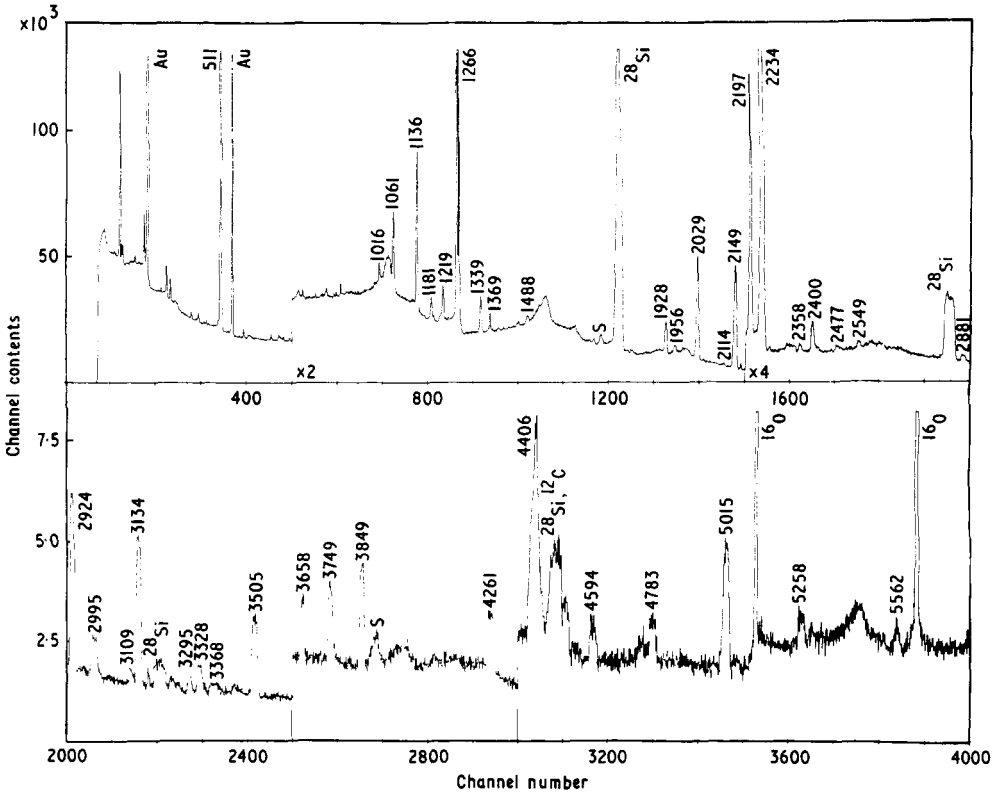

Figure 1. An escape-suppressed GeLi spectrum taken at a bombarding energy of 10·5 MeV, following the $^{28}Si(\alpha, p\gamma)^{31}P$ reaction. Gamma rays assigned to ^{31}P are marked in keV and other γ rays identified by the nucleus in which they originate, except the letter S indicates a single-escape peak.

centroid position against $\cos\theta$ data. The quantity F as a function of mean nuclear lifetime was calculated (Blaugrund 1966) using a program that took into account the stopping in the gold target backing. The errors in the lifetimes quoted in table 2 represent only errors associated with the measurement of the F factors. There is an additional uncertainty in the conversion of the F factors into lifetimes due to lack of full knowledge of the stopping theory involved. A reasonable figure for this uncertainty is plus or minus 25%.

2.2. Angular distribution and polarization measurements

These measurements were carried out simultaneously with the lifetime experiments. Gamma-ray yields were determined at each angle using the escape-suppressed spectrometer and normalized with respect to the yield in a GeLi detector fixed at $\theta = 90°$. Branching ratios were calculated from the normalization factors A_0 which were obtained by linear least-squares fits to the angular distributions

$$W(\theta) = \sum_k A_k Q_k P_k(\cos\theta)$$

where the solid angle correction factors Q_2 and Q_4 were taken as 0·995 and 0·980 respectively.

The γ-ray linear polarizations were measured with a 3 GeLi detector Compton polarimeter (Butler *et al* 1973), which had a polarization sensitivity varying from 0·50 at 0·7 MeV to 0·10 at 3 MeV. The relative efficiencies of the two absorbers were measured both before and after the experiments and the sensitivity of the instrument calibrated as described by Butler *et al* (1973). The definition of linear polarization was

$$P(\theta) = \frac{W(\theta, \phi = 0°) - W(\theta, \phi = 90°)}{W(\theta, \phi = 0°) + W(\theta, \phi = 90°)}$$

and the phase convention of Rose and Brink (1967) was adopted in the analysis.

The angular distribution and polarization data were used in three slightly different ways: (i) to establish the parity of the initial state when its spin and the mixing ratio of the relevant γ ray had previously been determined; (ii) to establish the spin and parity of the initial state and also the mixing ratio of the γ ray; and (iii) to measure the mixing ratio of a weak transition from a state of known spin when the mixing ratio of the major branch had already been determined. In the analysis for cases (i) and (iii) the alignment parameters are essentially established by the angular distributions of the major branch but for case (ii) some knowledge of the alignment parameters must be obtained from assumptions about the reaction mechanism. The experiments had been carried out using the (α, p) reaction on a spin-zero target approximately 300 keV thick such that the outgoing proton energy was 1–3 MeV in the centre of mass. The proton transmission coefficients are then approximately 0·4, 0·7, 0·02 and 0·0004 for transferred orbital angular momentum values of $l = 0, 1, 2$ and 3 respectively. Therefore, if we make the reasonable assumption that the reaction only proceeds very weakly through levels in the compound nucleus that require outgoing l values of $l \geqslant 2$ then only the two lowest magnetic substates can be strongly populated. Estimates of the populations of the substates were calculated using the compound nuclear statistical model (Sheldon and van Patter 1966) and gave average values of $P(\frac{1}{2}) = 0{\cdot}89$, $P(\frac{3}{2}) = 0{\cdot}20$, $P(\frac{5}{2}) = 0{\cdot}01$ and $P(\frac{7}{2}) = 0{\cdot}001$. We attempted to allow for errors arising from statistical fluctuations and deficiencies in the optical model used to calculate the transmission coefficients by

assuming an error of 50% in the estimated population of $P(\frac{3}{2})$, but substates $P(\frac{5}{2})$ and $P(\frac{7}{2})$, which have very small estimates, were fixed at zero population. This method of analysis was used for all 3 cases (i), (ii) and (iii) and the alignment data were included in the analysis following the techniques described by James *et al* (1974) whose method was used to calculate the errors on the mixing ratio.

2.3. Proton–gamma angular correlation measurements

Excited states of ^{31}P were populated using the $^{28}Si(\alpha, p\gamma)^{31}P$ reaction at α-particle bombarding energies of 17·00 and 17·06 MeV. Targets consisted of approximately 80 $\mu g\ cm^{-2}$ self-supporting ^{28}Si foils enriched to greater than 99·6%. The $^{28}Si(\alpha, \alpha')^{28}Si$ reaction has a large cross section and, hence, when a single annular particle detector was used the inelastic α-particle peaks masked many of the proton peaks of interest. In order to differentiate between α-particles and protons an annular particle detector telescope was developed. This consisted of a thin 50–70 μm totally depleted annular surface barrier counter (DE detector) placed 0·2 cm in front of a thick 1500 μm partially depleted annular counter (E detector) covering an annular range from 168°–174°. The DE detector was not thick enough to stop all α particles but a coincidence requirement between the two detectors coupled with a maximum limit on the pulse amplitude in the DE detector enabled all α particles to be rejected. The addition of the pulse amplitudes in the DE and E detectors resulted in an overall proton resolution of approximately 60 keV as shown in figure 2.

Angular correlations between the protons and the γ rays de-exciting the ^{31}P states were obtained by measuring the coincident γ-ray yield in five 5 in × 6 in NaI(Tl) crystals placed with their front faces 25 cm from the target at angles of 8°, 30°, 45°, 90° and 120°. Coincidence spectra between the protons and a GeLi detector placed 6 cm above the target at an angle of 90° were also recorded. These assisted in the identification of the decay modes of levels and confirmed that the peaks in the NaI spectra used for angular correlations contained only one γ ray. Conventional fast–slow electronics was used and each event digitized by particle energy, γ-ray energy deposited in the detector and the relative time separation between the detection of the particle and the γ ray. On-line analysis was carried out using a PDP7 computer to check that the experiment was proceeding satisfactorily and every event was written on magnetic tape for subsequent off-line analysis with an IBM 360/65 computer.

The methods used for the analysis of the angular correlations, rejection of spin hypotheses and errors on the multipole mixing ratios follow those described by James *et al* (1974) using the phase convention of Rose and Brink (1967).

3. Results

The decay modes of excited states were mainly established from the p–γ coincidence experiments but often the most accurate branching ratios were determined from the singles GeLi experiment. The mean values for the branching ratios, together with previous measurements, are quoted in table 1, which also contains spin assignments, lifetimes, multipole mixing ratios and γ-ray transition strengths. The attenuation factors F and the derived mean lifetimes are given in table 2, together with the previous measurements of De Voigt *et al* (1971) and Wolff *et al* (1968) who both used different reactions to excite the states in ^{31}P and hence had different velocities and slowing down

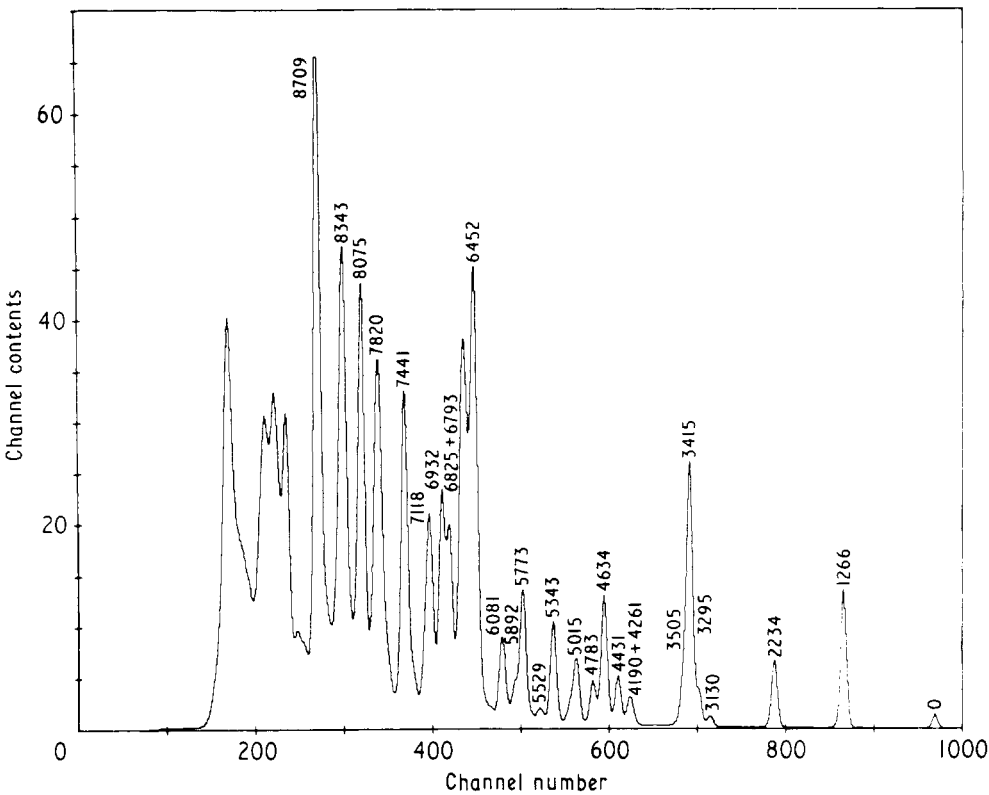

Figure 2. A proton spectrum from the reaction $^{28}Si(\alpha, p)^{31}P$ at $E_\alpha = 17{\cdot}0$ MeV. Alpha particles have been rejected as described in § 2.3 and excitation energies in ^{31}P are given in keV.

times for the recoiling ions. There is generally a good measure of agreement for those lifetimes that have been determined from all three reactions. However, we have obtained definite values for the lifetimes of several of the high spin states for which De Voigt *et al* only recorded limits and which Wolff *et al* did not excite.

In the following sections the results from the different experimental techniques are discussed only for individual levels or groups of levels for which new data are available. However table 3 contains the Legendre coefficients obtained from the angular distributions of all γ rays that were measured.

3.1. The 2234 keV state ($J^\pi = \frac{5}{2}^+$)

The experimental limit of a possible branch from the 2234 keV to 1266 keV states was fixed at less than 0·10% from the singles GeLi experiment at 10·5 MeV bombarding energy. This yields an E2 strength of less than 0·5 Wu assuming a pure quadrupole transition.

3.2. The 3295 keV state ($J^\pi = \frac{5}{2}^+$)

Although the decay modes of this state are well established there have been two conflicting measurements reported for the mixing ratio of the 1061 keV branch to the

Table 1. Present data on ^{31}P. The level energy is the mean value obtained from the present experiments except where no error is quoted and then the energy is obtained from previous work. The transition strengths are calculated from the lifetime and mixing ratio data given in columns 6 and 7. M1 strengths marked with a dagger (†) are calculated assuming δ is small as it has not been measured. The previous branching ratio measurements are from Wolff *et al* (1968) or De Voigt *et al* (1971) and in the cases where these do not add up to 100% in the table both the previous values and our upper limits are quoted in the discussion for individual levels in § 3.

Initial state		Final state								Branching ratio (%)	
E_x (keV)	J^π	E_γ (keV)	E'_x (keV)	J^π	τ_m (fs)	δ	$\lvert M(E2)\rvert^2$ (Wu)	$\lvert M(M1)\rvert^2$ (mWu)	$\lvert M(E1)\rvert^2$ (mWu)	Present	Previous
1266·1±0·4	$\frac{3}{2}^+$	1266	0	$\frac{1}{2}^+$	800±90	0·28±0·02	3·8±1·0	18±4		100	100
2233·6±0·4	$\frac{5}{2}^+$	2234	0	$\frac{1}{2}^+$	340±30	E2	7·3±0·7			100	100
		968	1266	$\frac{3}{2}^+$			≤0·5	≤0·1		≤0·1	≤0·8
3133·7±0·7	$\frac{1}{2}^+$	3134	0	$\frac{1}{2}^+$	≤15	M1		≥70		100	100
3294·8±0·5	$\frac{5}{2}^+$	2029	1266	$\frac{3}{2}^+$	117±20	−0·37±0·03	3·3±0·6	23±4		81±5	84±2
		1061	2234	$\frac{5}{2}^+$		−0·38±0·09	21±8	37±6		19±5	16±2
3414·6±0·6	$\frac{7}{2}^+$	2149	1266	$\frac{3}{2}^+$	320±30	E2	9·4±1·3			96±1	100
		1181	2234	$\frac{5}{2}^+$		0·35±0·07	0·8±0·3	2·1±0·5		4±1	
3505·4±0·7	$\frac{3}{2}^+$	3505	0	$\frac{1}{2}^+$	≤10	−0·40±0·03	≥2·3	≥40		64±4	62±4
		2239	1266	$\frac{3}{2}^+$				≥100†		36±4	38±4
4190·1±0·5	$\frac{5}{2}^+$	2924	1266	$\frac{3}{2}^+$	≤15	0·12±0·05	≥0·2	≥63		76±4	76±2
		1956	2234	$\frac{5}{2}^+$		−0·09±0·14		≥100		24±3	24±2
4261±1	$\frac{3}{2}^+$	4261	0	$\frac{1}{2}^+$	≤15	−0·40±0·06	≥0·4	≥15		64±4	75±3
		2995	1266	$\frac{3}{2}^+$		−0·25±0·05	≥0·5	≥27		36±4	25±3
4430·5±0·5	$\frac{7}{2}^-$	2197	2234	$\frac{5}{2}^+$		E1			0·07±0·01	45±4	55±2
		1136	3295	$\frac{5}{2}^+$	590±30	E1			0·56±0·06	49±4	41±2
		1016	3415	$\frac{7}{2}^+$		E1			0·10±0·01	6±2	4±1
4594·2±0·7	$\frac{3}{2}^+$	4594	0	$\frac{1}{2}^+$				2·7±1·3†		19±3	24±4
		3328	1266	$\frac{3}{2}^+$	23±13	0·8±0·4	3·5±2·5	14±7		62±4	54±5
		2360	2234	$\frac{5}{2}^+$				20±10†		19±3	22±6
4633·6±0·6	$\frac{7}{2}^+$	3368	1266	$\frac{3}{2}^+$		E2	0·10±0·03			3±1	
		2400	2234	$\frac{5}{2}^+$	100±15	−0·45±0·06	0·6±0·2	4·7±1·3		22±4	25±3
		1339	3295	$\frac{5}{2}^+$		−0·38±0·04	15±4	42±11		36±3	47±5
		1219	3415	$\frac{7}{2}^+$		−0·33±0·06	19±5	60±15		39±2	28±3

Table 1 (*continued*)

Initial state		Final state								Branching ratio (%)	
E_x (keV)	J^π	E_γ (keV)	E'_x (keV)	J^π	τ_m (fs)	δ	$\lvert M(E2)\rvert^2$ (Wu)	$\lvert M(M1)\rvert^2$ (mWu)	$\lvert M(E1)\rvert^2$ (mWu)	Present	Previous
4783·0±0·6	$\frac{5}{2}^+$	4783	0	$\frac{1}{2}^+$		E2	⩾1·7			46±4	42±3
		3517	1266	$\frac{3}{2}^+$						⩽8	12±3
		2549	2234	$\frac{5}{2}^+$	⩽15			⩾24†		19±3	15±3
		1488	3295	$\frac{5}{2}^+$		−0·04±0·10		⩾220†		35±4	31±3
5010	$\frac{3}{2}^-$	5015	0	$\frac{1}{2}^+$	70±15	E1			0·08±0·02	75±5	68±3
		3749	1266	$\frac{3}{2}^+$		E1			0·07±0·02	25±5	32±3
5020	$\frac{3}{2}^+(\frac{1}{2})$	5015	0	$\frac{1}{2}^+$	⩽10			⩾5†		20±10	40±3
		3749	1266	$\frac{3}{2}^+$				⩾45†		80±10	60±3
5115·2+0·7	$\frac{5}{2}^+$	3849	1266	$\frac{3}{2}^+$		−0·30±0·06	0·6±0·2	21±7		62±4	
		2881	2234	$\frac{5}{2}^+$	15±5	$-0·1 > \delta > -1·2$	3±3	15±6		25±4	
		1700	3415	$\frac{7}{2}^+$		$-0·6 > \delta > -2·7$	40±20	25±15		13±3	
5258±2	$\frac{1}{2}^+$	5258	0	$\frac{1}{2}^+$	⩽15	M1		⩾14		100	100
5343·1±0·6	$\frac{9}{2}^+$	3109	2234	$\frac{5}{2}^+$		E2	1·0±0·2			10±2	29±8
		2048	3295	$\frac{5}{2}^+$	48±10	E2	6·4±1·4			8±2	21±8
		1928	3415	$\frac{7}{2}^+$		−0·04±0·06	⩽0·9	74±15		82±4	50±10
5529±1	$\frac{7}{2}^+$	3295	2234	$\frac{5}{2}^+$	⩽15	−0·12±0·05				46±6	50±30
		2114	3415	$\frac{7}{2}^+$		−1·0±0·5	⩾25	⩾110		54±6	50±30
5562±2	$\frac{3}{2}^+$	5562	0	$\frac{1}{2}^+$						100	82
		3328	2234	$\frac{5}{2}^+$							18
5672	$\frac{5}{2}$	4406	1266	$\frac{3}{2}^+$						masked	55
		3438	2234	$\frac{5}{2}^+$						50	10
		2257	3415	$\frac{7}{2}^+$						50	10
		1241	4431	$\frac{7}{2}^-$						<10	10
5773±1	$(\frac{5}{2}, \frac{7}{2})$	3539	2234	$\frac{5}{2}^+$						25±8	15±5
		2358	3415	$\frac{7}{2}^+$						50±10	40±15
		1583	4190	$\frac{5}{2}^+$						15±5	
		1139	4634	$\frac{7}{2}^+$						10±5	25±10

Table 1 (*continued*)

Initial state		Final state								Branching ratio (%)	
E_x (keV)	J^π	E_γ (keV)	E'_x (keV)	J^π	τ_m (fs)	δ	$\lvert M(E2)\rvert^2$ (Wu)	$\lvert M(M1)\rvert^2$ (mWu)	$\lvert M(E1)\rvert^2$ (mWu)	Present	Previous
5892·4±0·7	$\frac{9}{2}^+$	3658	2234	$\frac{5}{2}^+$	30±9	E2	6·3±2·0			90±2	100
		2477	3415	$\frac{7}{2}^+$		−0·23±0·06	0·2±0·1	6·5±2·0		10±2	
5988		4722	1266	$\frac{3}{2}^+$						100	
6048±1	$\frac{7}{2}^+$	3814	2234	$\frac{5}{2}^+$		1·7 > δ > 0·6	0·6±0·3	2±1		22±4	
		2633	3415	$\frac{7}{2}^+$	32±15	0·2 > δ > −1·0	≤10	20±9		51±4	
		1414	4634	$\frac{7}{2}^+$				90±40†		27±6	
6081±1	$\frac{9}{2}^+$	3847	2234	$\frac{5}{2}^+$	32±15	E2	4·5±2·0			88±3	100
		1447	4634	$\frac{7}{2}^+$				38±17†		12±3	
6398±1	$\frac{7}{2}^{(-)}$	1967	4431	$\frac{7}{2}^-$	32±15	0·03±0·08	≤1·7	130±50		100	
6452±1	$\frac{11}{2}^+$	3037	3415	$\frac{7}{2}^+$	32±15	E2	15±6			89±4	90±10
		1109	5343	$\frac{9}{2}^+$		−0·27±0·03	26±10	70±30		11±4	
6500±1	$\frac{9}{2}^-$	3085	3415	$\frac{7}{2}^+$	55±15	E1			0·15±0·04	25±5	50±20
		2069	4431	$\frac{7}{2}^-$		−1·3±0·3	31±11	18±6		75±5	50±20
6793±1	$\frac{9}{2}^-$	3378	3415	$\frac{7}{2}^+$	200±30	E1			0·03±0·01	25±8	
		2362	4431	$\frac{7}{2}^-$		0·29±0·04	0·5±0·1	8±1		75±8	
6825±1	$\frac{11}{2}^-$	2394	4431	$\frac{7}{2}^-$	90±30	E2	12±4			60±10	60±15
		1482	5343	$\frac{9}{2}^+$		E1			1·4±0·4	40±10	
6932	$\frac{5}{2}^+$	4698	2234	$\frac{5}{2}^+$	≤40	1·3±0·3				100	<100
7080		2649	4431	$\frac{7}{2}^-$						100	
7118±1	$\frac{9}{2}^+$	3703	3415	$\frac{7}{2}^+$	≤25	0·18±0·02	≥0·2	≥24		100	
7441±1	$\frac{11}{2}^+$	4026	3415	$\frac{7}{2}^+$	≤15	E2	≥8			91±2	40±10
		989	6452	$\frac{11}{2}^+$		−0·3±0·3		≥180		9±2	
7466±2		4051	3415	$\frac{7}{2}^+$						45±10	
		3035	4431	$\frac{7}{2}^-$						45±10	
		966	6500	$\frac{9}{2}^-$						10±5	

Table 2. The measured F factors and derived mean lifetimes from the present work compared with the previous determinations of Wolff *et al* (1968) and De Voigt *et al* (1971).

Level energy (keV)	E_γ (keV)	E_α (MeV)	F factor	F factor average	τ_m (fs)		
					Present experiment†	De Voigt *et al*	Wolff *et al*
1266	1266	6·75	0·36 ± 0·03	0·36 ± 0·03	800 ± 90		770 ± 150
2234	2234	6·75	0·60 ± 0·02	0·60 ± 0·02	340 ± 30		425 ± 30
3134	3134	8·5	0·99 ± 0·01	⩾0·98	⩽15		8 ± 4
		10·5	1·03 ± 0·02				
3295	2029	8·5	0·85 ± 0·01	0·85 ± 0·01	117 ± 20	130 ± 50	135 ± 14
3415	2149	8·5	0·64 ± 0·01	0·64 ± 0·01	320 ± 30	300 ± 80	320 ± 60
3505	3505	10·5	1·00 ± 0·01	⩾0·99	⩽10		13 ± 7
4190	2924	10·5	1·02 + 0·02	⩾0·98	⩽15	⩽40	⩽23
	1956		1·00 ± 0·03				
4261	4261	10·5	1·01 ± 0·02	⩾0·98	⩽15		15 ± 5
	2995		1·09 ± 0·04				
4431	1136	10·5	0·50 ± 0·01	0·49 ± 0·01	590 ± 30	⩾300	1200 ± 500
	1016		0·44 ± 0·04				
4594	4594	10·5	0·96 ± 0·04	0·97 ± 0·02	23 ± 13		44 ± 19
	3328		0·98 ± 0·02				
4634	2400	10·5	0·85 ± 0·02				
	1339		0·86 ± 0·01	0·86 ± 0·01	110 ± 15	90 ± 20	100 ± 30
	1219		0·90 ± 0·02				
4783	4783	10·5	1·01 ± 0·01	⩾0·98	⩽15	90 ± 50	14 ± 11
	2549		0·99 ± 0·03				
5115	3849	10·5	0·98 ± 0·01	0·98 ± 0·01	15 ± 5		
5258	5258	10·5	1·02 ± 0·03	⩾0·98	⩽15		
5343	1928	10·5	0·94 ± 0·01	0·94 ± 0·01	48 ± 10	⩽30	
5529	3295	10·5	1·00 ± 0·02	⩾0·98	⩽15		
	2114		1·01 ± 0·03				
5892	3658	10·5	0·96 ± 0·01	0·96 ± 0·01	30 ± 9	⩽90	80 ± 60
6048	3814	12·0	0·95 ± 0·05	0·96 ± 0·02	32 ± 15		
	2633		0·96 ± 0·02				
6081	3847	12·0	0·95 ± 0·02	0·96 ± 0·02	32 ± 15	⩽60	

Table 3. Coefficients of Legendre polynomials corrected for solid angle effects. Bombarding energies, E_α, of 17·00 and 17·06 MeV refer to data from NaI p–γ coincidence experiments and E_α = 10·5, 12·0 and 14·0 MeV refer to angular distributions from the singles GeLi experiments.

E_x (keV)	E_γ (keV)	E_α (MeV)	a_2	a_4	E_x (keV)	E_γ (keV)	E_α (MeV)	a_2	a_4
3295	1061	10·5	0·61 ± 0·02	0·05 ± 0·02	5529	2114	10·5	0·53 ± 0·011	−0·35 ± 0·12
	2029	10·5	0·26 ± 0·01	0·04 ± 0·02		3295	10·5	−0·09 ± 0·09	0·01 ± 0·12
3415	1181	10·5	0·90 ± 0·05	0·05 ± 0·05	5892	3658	17·06	0·42 ± 0·03	−0·29 ± 0·03
3505	3505	17·06	0·27 ± 0·02	−0·03 ± 0·03		2234	17·06	0·41 ± 0·06	−0·26 ± 0·07
4190	2924	17·06	−0·64 ± 0·05	0·05 ± 0·06		2477	12·0	0·15 ± 0·12	0·03 ± 0·14
	1956	10·5	0·47 ± 0·07	0·18 ± 0·05	6048	2633	12·0	0·47 ± 0·09	−0·03 ± 0·12
4261	4261	17·06	0·23 ± 0·04	0·05 ± 0·05		3814	12·0	−1·03 ± 0·17	0·36 ± 0·20
4594	3328	17·06	0·41 ± 0·04	0·03 ± 0·05	6081	3847	17·06	0·46 ± 0·02	−0·30 ± 0·02
4634	1219	10·5	0·64 ± 0·02	−0·02 ± 0·02		2234	17·06	0·38 ± 0·04	−0·28 ± 0·05
	1339	10·5	0·42 ± 0·03	0·09 ± 0·03	6398	1967	12·0	0·42 ± 0·04	0·01 ± 0·05
	2400	10·5	0·47 ± 0·04	0·09 ± 0·05	6452	1109	12·0	0·21 ± 0·04	0·04 ± 0·04
4783	1488	17·06	0·50 ± 0·05	−0·02 ± 0·06		3037	17·06	0·42 ± 0·02	−0·23 ± 0·02
5015(D)	3749	10·5	0·21 ± 0·04	0·00 ± 0·04		2149	17·06	0·50 ± 0·03	−0·17 ± 0·03
	3749	12·0	0·12 ± 0·06	0·05 ± 0·07	6500	2069	12·0	0·92 ± 0·05	0·39 ± 0·06
	5015	10·5	−0·31 ± 0·03	0·01 ± 0·04	6793	2362	12·0	−0·82 ± 0·05	0·08 ± 0·06
	5015	12·0	−0·22 ± 0·17	0·33 ± 0·20		3378	17·06	−0·32 ± 0·03	0·02 ± 0·04
5115	1700	10·5	−1·01 ± 0·26	0·13 ± 0·33	6825	1482	17·00	−0·31 ± 0·10	0·01 ± 0·11
	2881	10·5	0·55 ± 0·06	−0·02 ± 0·07		1482	14·0	−0·53 ± 0·04	0·07 ± 0·05
	3849	10·5	0·20 ± 0·30	−0·06 ± 0·04	6932	4698	17·06	−0·52 ± 0·02	−0·18 ± 0·02
5258	5258	17·06	0·11 ± 0·04	0·01 ± 0·05	7118	3703	17·06	−0·67 ± 0·01	0·06 ± 0·01
5343	1928	10·5	−0·42 ± 0·02	0·07 ± 0·03		2149	17·06	0·51 ± 0·02	−0·21 ± 0·02
	1928	17·00	−0·24 ± 0·05	0·06 ± 0·06	7441	989	14·0	0·81 ± 0·08	−0·19 ± 0·09
	2149	17·00	0·47 ± 0·05	−0·29 ± 0·05		4026	17·06	0·45 ± 0·03	−0·24 ± 0·04
						2149	17·06	0·43 ± 0·03	−0·15 ± 0·04

3.3. The 3415 keV state ($J^\pi = \frac{7}{2}^+$)

Previous work had only reported a 100% decay to the 1266 keV ($\frac{3}{2}^+$) state. However, the present singles GeLi spectra contain a 1181 keV γ ray showing that there is a 4 ± 1% branch to the 2234 keV ($\frac{5}{2}^+$) state. The strongly anisotropic angular distribution of this weak branch, shown in figure 3(*a*), was fitted together with that of the 2149 keV γ ray, which fixed the alignment, and yielded a multipole mixing ratio of +0·35 ± 0·07.

3.4. The 4431 keV state ($J^\pi = \frac{7}{2}^-$)

We report a measurement of 590 ± 30 fs for the lifetime of this state, considerably faster than the value of 1·2 ± 0·5 ps obtained by Wolff *et al* (1968) from a (p, γ) experiment. The present measurement is more accurate due to the much higher recoil velocities in the (α, p) experiment yielding a larger F value 0·49 ± 0·01 compared with 0·09 ± 0·04 from the (p, γ) work.

3.5. The 4634 keV state ($J^\pi = \frac{7}{2}^+$)

Previous work had been unable to distinguish between spin assignments of $\frac{5}{2}^+$ and $\frac{7}{2}^+$ for this state, which decays to the 3415 ($\frac{7}{2}^+$), 3295 ($\frac{5}{2}^+$) and 2234 keV ($\frac{5}{2}^+$) states. In the

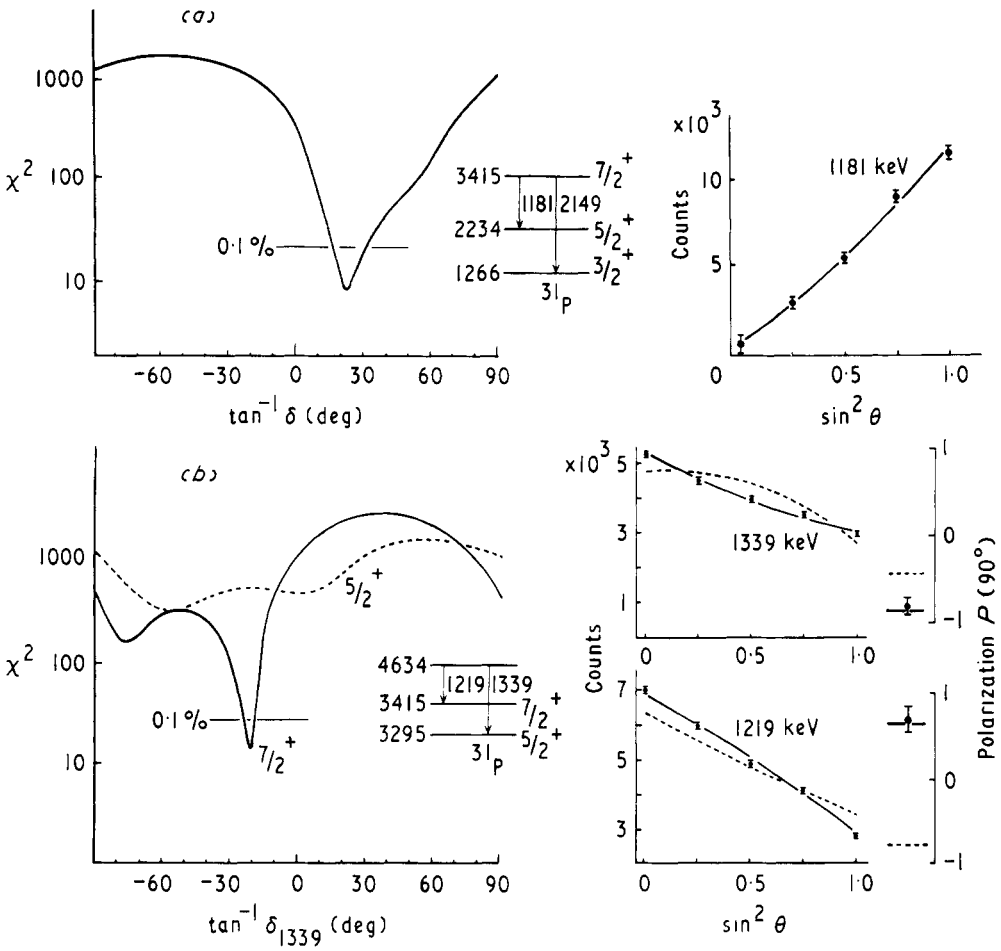

Figure 3. (*a*) The 3415 keV state: the angular distribution of the small 4% branch to the 2234 keV state and the χ^2 plot that results in a mixing ratio of $+0{\cdot}35 \pm 0{\cdot}07$ for the 1181 keV γ ray. (*b*) The 4634 keV state: the angular distributions and polarizations of the 1219 and 1339 keV γ rays which were fitted simultaneously to give the χ^2 plots shown that indicate the spin of the state is $\frac{7}{2}^+$ and the mixing ratio of the 1339 keV transition is $-0{\cdot}38 \pm 0{\cdot}04$.

p–γ coincidence experiment the γ rays from the decay of the state are degenerate in the NaI detectors but they are clearly resolved and strongly excited in the singles GeLi measurements. This latter fact enabled accurate polarization values of $0{\cdot}69 \pm 0{\cdot}15$ (1219 keV) and $-0{\cdot}81 \pm 0{\cdot}10$ (1339 keV) to be measured for the two major branches. The angular distributions and polarizations for both γ rays were fitted simultaneously, with the alignment parameters treated as in § 2.2, and the only acceptable fit to the data was given by the $\frac{7}{2}^+$ assignment, as shown in figure 3(*b*). The mixing ratios of both major branches, established from this analysis, were almost identical; $-0{\cdot}38 \pm 0{\cdot}04$ and $-0{\cdot}33 \pm 0{\cdot}06$ for the 1339 keV and 1219 keV transitions respectively. The mixing ratio of the weaker 2400 keV branch to the 2234 keV ($\frac{5}{2}^+$) state was determined by simultaneously fitting the angular distributions of the 1219 and 2400 keV transitions and the 1219 keV polarization. This yielded a mixing ratio of $-0{\cdot}45 \pm 0{\cdot}06$.

The present branching fractions for the state clearly show that the major branches have almost equal strength in disagreement with the previous conclusion of Wolff *et al* (1968) that the 1339 keV branch was much the stronger. We also report a new $3 \pm 1\%$ branch to the 1266 keV ($\frac{3}{2}^+$) state from the singles GeLi spectra at 10·5 MeV.

3.6. The 5015 keV doublet ($J^\pi = \frac{3}{2}^-$ and $\frac{3}{2}^+(\frac{1}{2})$)

At this excitation energy two states separated by less than 0·5 keV were identified by Wolff *et al* (1968) from different branching ratio measurements to the ground and 1266 keV states at four (p, γ) resonances (ground state fractions of $68 \pm 3\%$, $68 \pm 10\%$, $38 \pm 3\%$ and $44 \pm 3\%$) and different lifetime measurements (67 ± 11 fs and 10 ± 7 fs) at two of the resonances. We obtained a 45% branch to the ground state at $E_\alpha = 10{\cdot}5$ MeV and only 20% at $E_\alpha = 12$ MeV, with different lifetimes for the two γ-ray branches at the lower energy, whereas Wolff *et al* recorded similar measurements for the two γ rays at each resonance. The data on the doublet are presented in table 4 where we have calculated lifetimes for each γ ray at the two (p, γ) resonances from the published F values of Wolff *et al*. We conclude that Wolff *et al* were incorrect in assuming each resonance exclusively fed only one member of the doublet and we estimate that the branching fractions to the ground state for individual members of the doublet are $75 \pm 5\%$ (5·01 MeV) and $20 \pm 10\%$ (5·02 MeV). We have taken the lifetimes of the two states to be 70 ± 15 fs and less than 10 fs.

One member of the doublet is expected to have $J^\pi = \frac{3}{2}^-$ from (d, n) work (Cujec *et al* 1965) and Wolff *et al* are able to restrict the spin assignments to $\frac{3}{2}(\frac{1}{2}^-)$ for the lower 5·01 MeV member and to $\frac{1}{2}(\frac{3}{2}^+)$ for the upper 5·02 MeV member. We obtain an anisotropic angular distribution for the 5015 keV γ ray at $E_\gamma = 10{\cdot}5$ MeV (see table 3) excluding the $J = \frac{1}{2}$ possibility for the 5·01 MeV state and obtain an a_2 coefficient consistent with a pure dipole transition and, therefore, conclude that $J^\pi = \frac{3}{2}^-$ for this state. Table 3 also shows that the angular distributions for the 5·02 MeV state indicate some anisotropy and so we favour the $\frac{3}{2}^+$ assignment for this state.

3.7. The 5115 keV state ($J^\pi = \frac{5}{2}^+$)

This state has been previously observed by Moss (1969) but its decay modes had not been established. We observed branches to the 1266 keV ($\frac{3}{2}^+$) state ($64 \pm 3\%$), the

Table 4. The branching ratio and lifetime data on the 5015 keV doublet from the present $^{28}Si(\alpha, p\gamma)^{31}P$ experiment and the previous $^{30}Si(p, \gamma)^{31}P$ experiment of Wolff *et al* (1968). The estimated data for the two individual levels is also given.

Reaction	Bombarding energy (MeV)	$E_\alpha = 5015$ keV		$E_\gamma = 3749$ keV	
		Branching ratio (%)	τ_m (fs)	Branching ratio (%)	τ_m (fs)
(α, pγ)	$E_\alpha = 10{\cdot}5$	45 ± 4	55 ± 10	55 ± 4	$\leqslant 10$
	$E_\alpha = 12$	20 ± 6	$\leqslant 15$	80 ± 6	$\leqslant 10$
(p, γ)	$E_p = 1{\cdot}298$	68 ± 3	67 ± 11	32 ± 3	50 ± 30
	$E_p = 1{\cdot}490$	44 ± 3	13^{+14}_{-8}	56 ± 3	6^{+10}_{-6}
Estimate	$E_x = 5{\cdot}01$	75 ± 5	70 ± 15	25 ± 5	70 ± 15
	$E_x = 5{\cdot}02$	20 ± 10	$\leqslant 10$	80 ± 10	$\leqslant 10$

2234 keV ($\frac{5}{2}^+$) state ($26 \pm 3\%$) and to the 3415 keV ($\frac{7}{2}^+$) state ($10 \pm 2\%$) from the singles GeLi experiment at 10·5 MeV. The angular distributions were anisotropic, ruling out $J = \frac{1}{2}$; the $J = \frac{7}{2}$ assignment did not fit either the distribution of the 3849 keV major branch or that of the weak 1700 keV branch; this latter distribution was also far too anisotropic for a transition from a $\frac{3}{2}$ state. We therefore conclude that the spin of the 5115 keV state is $\frac{5}{2}$ and the mixing ratios, given in table 1, are significantly nonzero which with the measured lifetime of 15 ± 5 fs rule out the M2 solutions fixing the parity of the state as positive.

3.8. The 5343 keV state ($J^\pi = \frac{9}{2}^+$)

The branching ratios for the 5343 keV state measured from the singles GeLi angular distributions indicated a much larger branch of $82 \pm 4\%$ to the 3415 keV ($\frac{7}{2}^+$) state than the $50 \pm 10\%$ reported by Wolff *et al* (1968). The intensities of the other two branches were therefore quite weak and the coincidence NaI spectrum, shown in figure 4(*a*) was analysed ignoring these branches. A simultaneous fit to the 1928 and 2149 keV γ rays enabled the $J = \frac{3}{2}$ and $\frac{7}{2}$ solutions to be rejected ($\chi^2 > 40$; $\chi^2_{0.1\%} = 22$) but the data were equally well fitted by both the other assignments of $J = \frac{5}{2}$ and $\frac{9}{2}$ ($\chi^2 = 12$) at mixing ratios close to zero. This ambiguity was resolved by the polarization measurement of the 1928 keV γ ray together with its angular distribution at 10·5 MeV bombarding energy. These data, shown in figure 5, were fitted together with alignment data (as discussed in § 2.2) and the mixing ratios established in the previous analysis, for both $J^\pi = \frac{5}{2}^+$ and $\frac{9}{2}^+$. The resulting χ^2 plots in figure 5 show that the 5343 keV state can be assigned $J^\pi = \frac{9}{2}^+$ and the mixing ratio of the 1928 keV γ ray is essentially dipole. The lifetime of the state was measured to be 48 ± 10 fs which also enables the $\frac{9}{2}^-$ possibility to be rejected due to unacceptable M2 strengths of 30 and 220 Wu for the smaller branches.

3.9. The 5529 keV state ($J^\pi = \frac{7}{2}^+(\frac{5}{2}^+)$)

The 5529 keV state was weakly excited in the proton–gamma coincidence experiment but the spectra indicated branches to the 2234 ($\frac{5}{2}^+$) and 3415 ($\frac{7}{2}^+$) keV states. This was confirmed by the singles GeLi experiment and the branching fraction to the 2234 keV state measured as $46 \pm 6\%$, in good agreement with previous data (see table 1). The angular distribution of the 2114 keV γ ray to the 3415 keV state can be fitted with $J = \frac{7}{2}$ at $\delta = -1{\cdot}0$ ($\chi^2 = 4{\cdot}3$) but the $J = \frac{5}{2}$ assignment can only be rejected at the 1% confidence limit ($\chi^2 = 12$). We, therefore, strongly favour the $\frac{7}{2}$ assignment consistent with the previous conclusion of Wolff *et al* (1968) that $J = \frac{7}{2}(\frac{5}{2}^+)$. The lifetime of 15 fs or less would give an M2 strength of 1200 Wu or more ruling out negative parity for the $\frac{7}{2}$ assignment.

3.10. The 5672 keV and 5773 keV states

The 5672 keV state was very weakly excited in the proton–gamma coincidence experiment but the previously established decays to the 2234 and 3415 keV states were observed in the singles GeLi experiment. There was no evidence of a decay to the 4431 keV ($\frac{7}{2}^-$) state as previously reported and the main decay mode to the 1266 keV state was completely masked by other γ rays.

The 5773 keV state was also weakly excited in the proton–gamma coincidence experiment and in the GeLi singles experiment the main primary γ rays were masked.

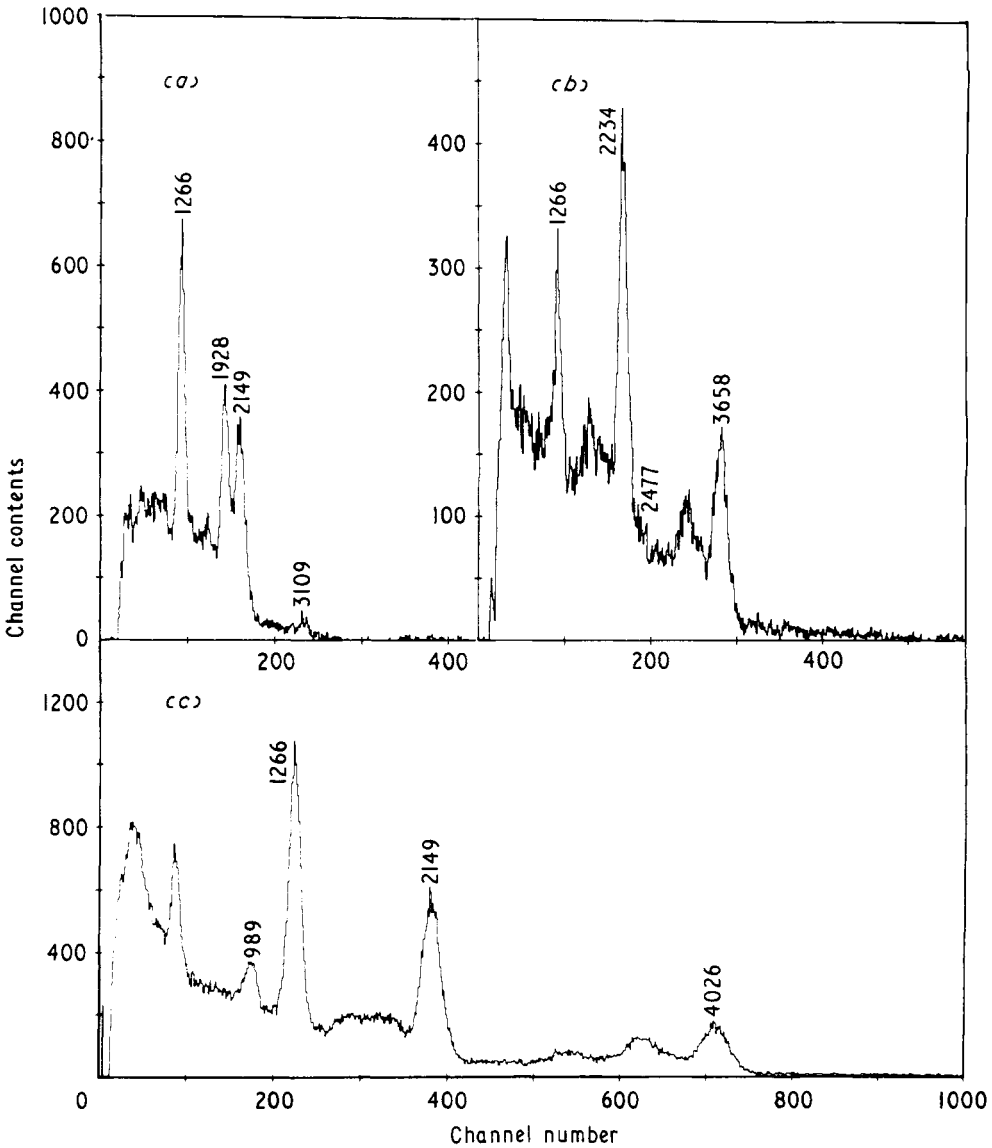

Figure 4. Gamma-ray spectra obtained from the NaI(Tl) detectors in coincidence with protons exciting the (*a*) 5343 keV state, (*b*) the 5892 keV state, and (*c*) the 7441 keV state in ^{31}P.

However, we did not observe the $20 \pm 10\%$ branch to the 1266 keV state reported by De Voigt *et al* (1971) and place an upper limit of 10% on this decay but do propose a new $15 \pm 5\%$ branch via a 1583 keV γ ray to the 4190 keV ($\frac{5}{2}^+$) state.

3.11. The 5892 keV state ($J^\pi = \frac{9}{2}^+$)

The NaI spectrum from the proton–gamma experiment (figure 4(*b*)) shows that the major decay is to the 2234 keV ($\frac{5}{2}^+$) state via a 3658 keV γ ray. A γ ray of about 2·5 MeV

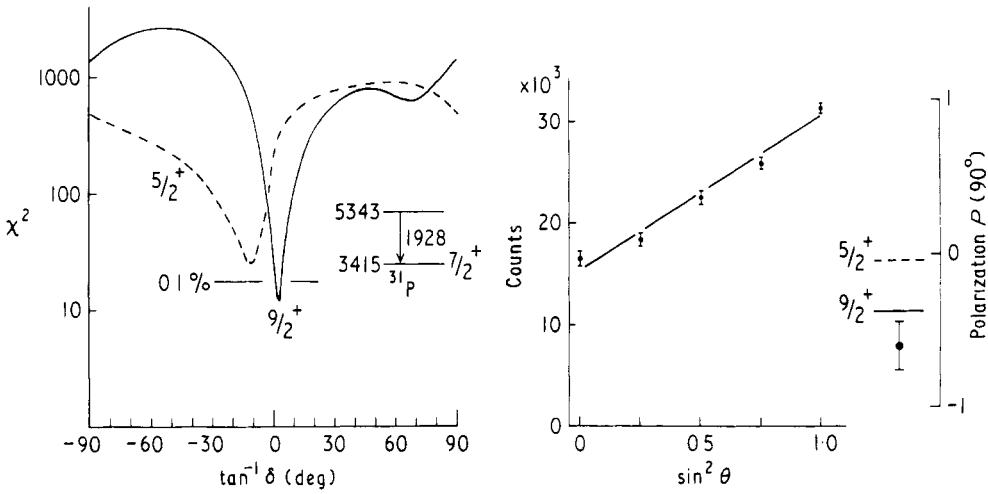

Figure 5. The 5343 keV state: the angular distribution and polarization of the 1928 keV γ ray at $E_\alpha = 10{\cdot}5$ MeV with the χ^2 plots that show the 5343 keV state has $J^\pi = \frac{9}{2}^+$.

is also observed together with the 1266 keV transition indicating a weak branch to the 3415 keV ($\frac{7}{2}^+$) state. This is confirmed by the singles GeLi experiment and the 2477 keV branching fraction measured to be $10 \pm 2\%$. The weak branch was ignored in the analysis to obtain angular distributions of the 3658 and 2234 keV γ rays (figure 6(*a*)) which were fitted simultaneously enabling the 5892 keV state to be assigned $J = \frac{9}{2}$. The lifetime measurement of 30 ± 9 fs would yield an M2 strength of 220 ± 70 Wu which can be rejected fixing the parity of the state as positive. The angular distribution of the 2477 keV γ ray in the singles GeLi experiment has an a_2 of $0{\cdot}15 \pm 0{\cdot}12$ which results in an estimate of the mixing ratio of $-0{\cdot}23 \pm 0{\cdot}06$.

3.12. The 6048 keV ($J^\pi = \frac{7}{2}^+$) and 6081 keV ($J^\pi = \frac{9}{2}^+$) states

The decay modes of both these states were measured from the singles GeLi experiment. The 6081 keV state decays predominately to the 2234 keV ($\frac{5}{2}^+$) state with a small $12 \pm 3\%$ branch to the 4634 keV ($\frac{7}{2}^+$) state. The 6048 keV state has a main decay mode of 51% to the 3415 keV ($\frac{7}{2}^+$) state and two smaller branches of $27 \pm 6\%$ and $22 \pm 4\%$ to the 4634 keV and 2234 keV states respectively. In the proton–gamma coincidence experiment the NaI and GeLi spectra indicate that the 6081 keV state is very strongly excited compared with the 6048 keV state and hence the angular distributions of both the 3847 and 2234 keV γ rays (shown in figure 6(*b*)) could be used to establish the spin of the 6081 keV state. The χ^2 plots of figure 6(*b*) show this is $\frac{9}{2}$ and the measured lifetime of 32 ± 15 fs, which would yield an M2 strength of 150 ± 60 Wu, fixes the parity of the state as positive.

The angular distributions of all three branches from the 6048 keV state were obtained from the singles GeLi experiment and analysed as described in § 2.2. The distribution of the 3814 keV primary transition could only be fitted by $J = \frac{7}{2}$ ($\chi^2 = 2{\cdot}5$, $\chi^2_{0{\cdot}1\%} = 16$), the other spin possibilities being rejected with $\chi^2 > 25$. The measured lifetime of the state 32 ± 15 fs, together with the mixing ratio $1{\cdot}7 > \delta > 0{\cdot}6$, gives an M2 strength of at least 10 Wu which is unlikely and suggests the state has positive parity.

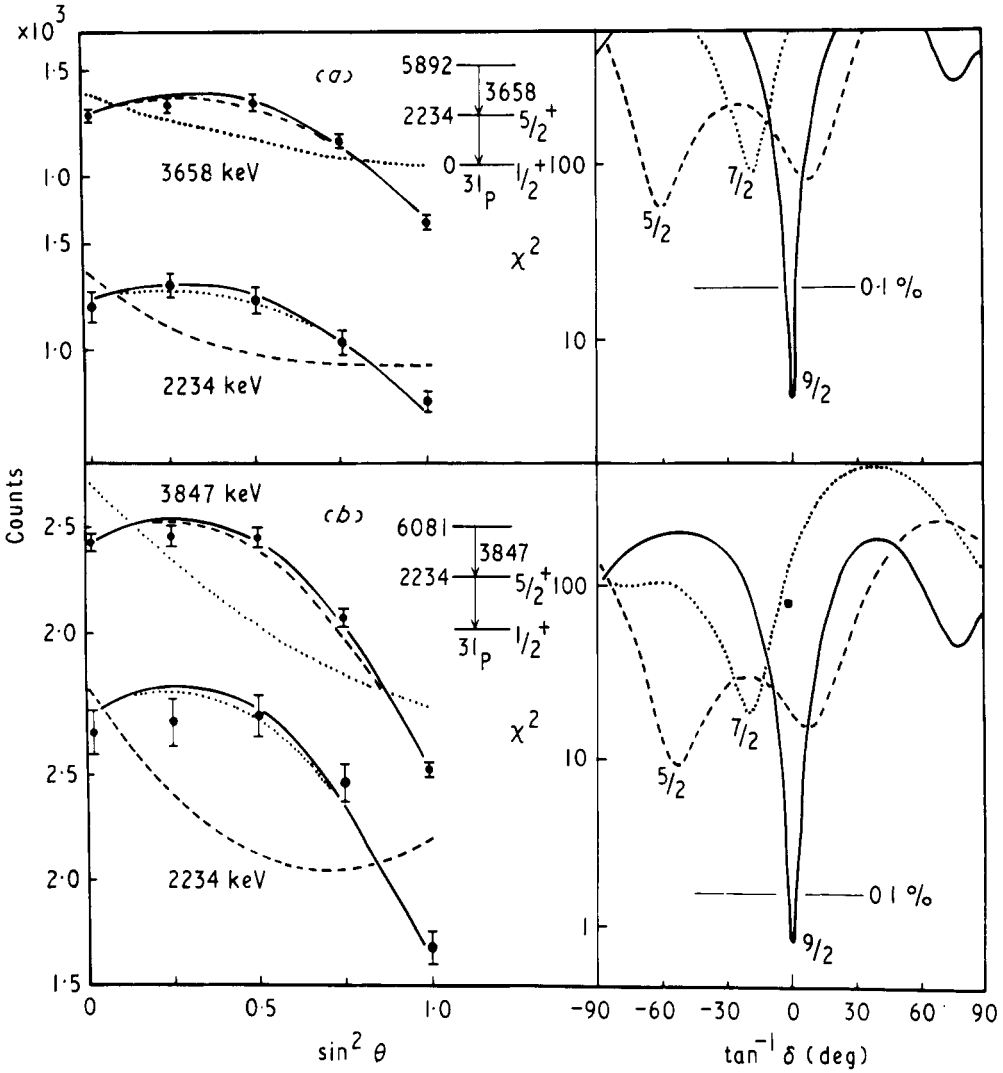

Figure 6. (*a*) The 5892 keV state: the angular distributions of the 3658 and 2234 keV γ rays from the proton–gamma coincidence experiment with the χ^2 plots indicating the state has $J = \frac{9}{2}$. (*b*) The 6081 keV state: angular distributions of the 3847 and 2234 keV γ rays from the p–γ coincidence experiment with the χ^2 plots indicating the 6081 keV state has $J = \frac{9}{2}$.

3.13. The 6398 keV state ($J^\pi = \frac{7}{2}^{(-)}$)

The 6398 keV state was only weakly excited in the proton–gamma coincidence experiment but the major decay mode reported by Wolff *et al* (1968) was observed in the singles GeLi experiment at 12 MeV. The analysis of the angular distribution yielded a mixing ratio of $+0{\cdot}03 \pm 0{\cdot}08$ in agreement with the value of $+0{\cdot}16 \pm 0{\cdot}14$ obtained by Wolff *et al*. We further suggest that this state is a good candidate to have negative parity due to its main decay mode to the 4431 keV ($\frac{7}{2}^-$) state.

3.14. The 6452 keV ($J^\pi = \frac{11}{2}^+$) and 6500 keV ($J^\pi = \frac{9}{2}^-$) states

The major decay of the 6452 keV state is to the 3415 keV ($\frac{7}{2}^+$) state via a 3037 keV γ ray. The GeLi coincidence spectrum also shows a weak branch of $11 \pm 4\%$ to the 5343 keV ($\frac{9}{2}^+$) state via a 1109 keV γ ray but there was no evidence for the $10 \pm 10\%$ branch to the 2234 keV ($\frac{5}{2}^+$) state proposed by De Voigt *et al* (1971) and we estimate such a branch must be no more than 5%. The spectra also showed that the nearby level at 6500 keV was only very weakly excited in the proton–gamma coincidence experiment and hence the angular distributions of all three γ rays in the main decay mode of the 6452 keV state were used in the subsequent analysis. The resulting χ^2 plots, shown in figure 7(*a*) enable an unambiguous spin assignment of $\frac{11}{2}$ to be made. The measured lifetime of 32 ± 15 fs would give an unacceptable M2 transition strength of 480 ± 180 Wu, hence showing the 6452 keV state has positive parity. The angular distribution of the small 1109 keV branch was obtained from the singles GeLi experiment and from the subsequent analysis, shown in figure 8(*a*), the mixing ratio determined to be $-0{\cdot}27 \pm 0{\cdot}03$.

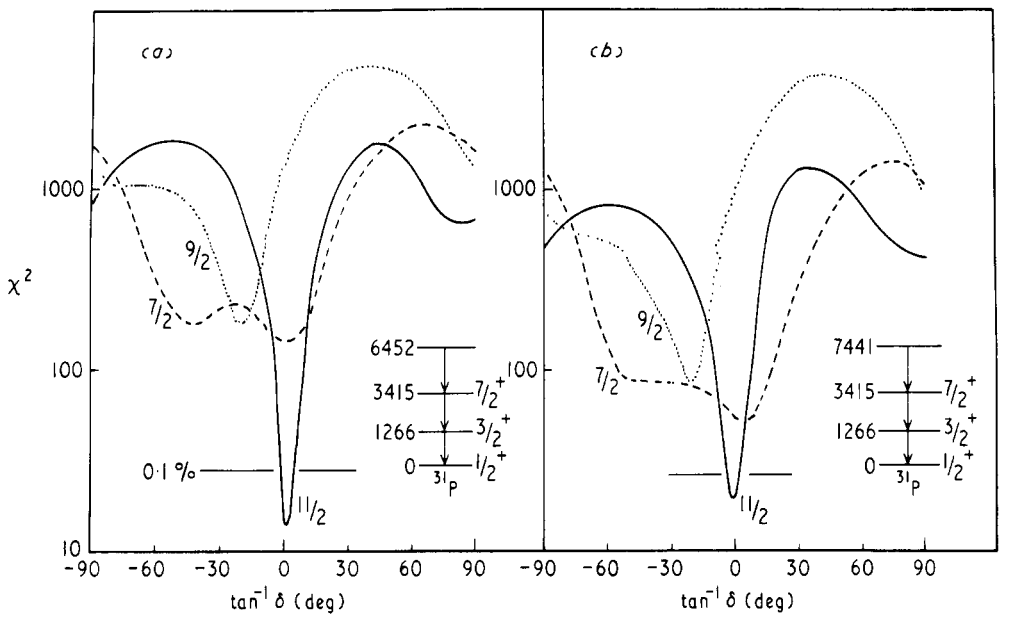

Figure 7. The χ^2 plots resulting from fitting all three γ rays in the cascade for (*a*) the 6452 keV state and (*b*) the 7441 keV state which show that in both cases the spin of the state is $\frac{11}{2}$.

The branching ratios of the 6500 keV state were measured in the 12 MeV singles GeLi experiment to be $75 \pm 5\%$ to the 4431 keV ($\frac{7}{2}^-$) state and $25 \pm 5\%$ to the 3415 keV ($\frac{7}{2}^+$) state. The angular distribution of the major 2069 keV transition could only be fitted with a spin assignment of $J = \frac{9}{2}$, as shown in figure 8(*b*), and established the mixing ratio as $-1{\cdot}3 \pm 0.3$. The parity of the state must be negative as the measured lifetimes of 55 ± 15 fs would give an unacceptable M2 transition strength of greater than 800 Wu. The angular distribution of the weaker branch was consistent with that expected from pure electric dipole radiation.

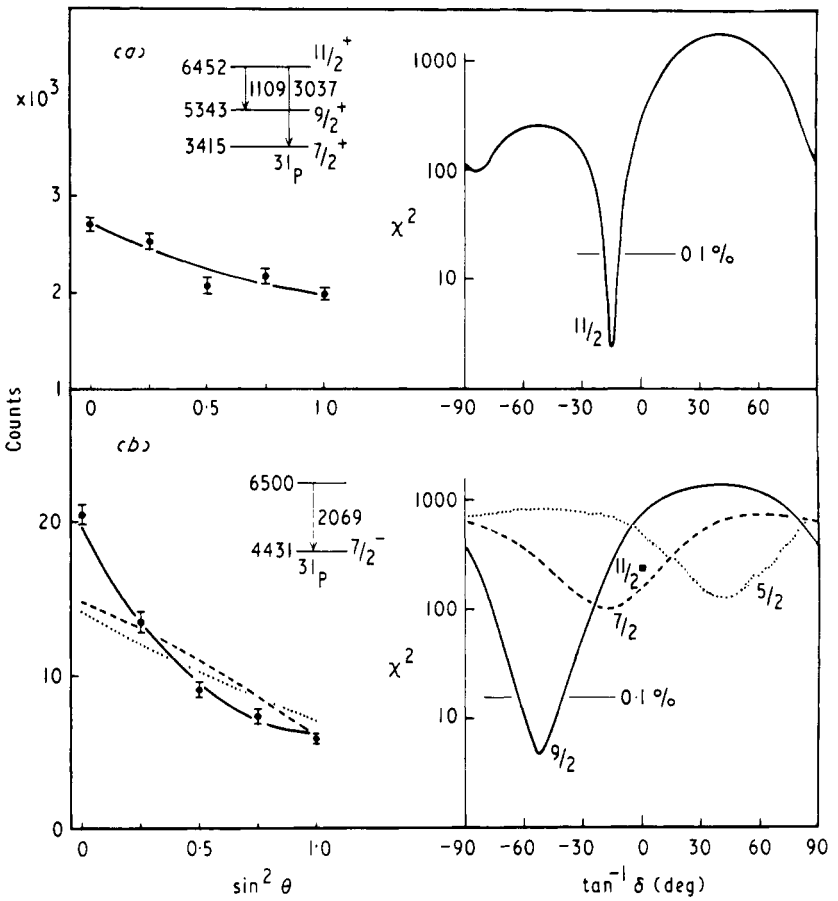

Figure 8. (*a*) The 6452 keV state: the angular distribution of the 1108 keV γ ray from the 11% branch to the 5343 keV state in the singles experiment at $E_\alpha = 12$ MeV with the χ^2 plot for $J = \frac{11}{2}$ that fixes the mixing ratio as $-0{\cdot}27 \pm 0{\cdot}03$. (*b*) The 6500 keV state: the angular distribution of the major 2069 keV branch from the 6500 keV state in the singles experiment at $E_\alpha = 12$ MeV with the associated χ^2 plot that shows the spin of the state is $J = \frac{9}{2}$.

3.15. The 6793 keV ($J^\pi = \frac{9}{2}^-$) and 6825 keV ($J^\pi = \frac{11}{2}^-$) states

In the proton–gamma coincidence experiment the 6793 keV state was preferentially excited at $E_\alpha = 17{\cdot}06$ MeV and the 6825 keV state at $E_\alpha = 17{\cdot}00$ MeV. The decay modes of each state were established from the GeLi coincidence spectra but measured more accurately in the singles GeLi experiment. The major decay of the 6793 keV state is via a 2362 keV γ ray to the 4431 keV ($\frac{7}{2}^-$) state, with a smaller 25 ± 8% branch to the 3415 keV ($\frac{7}{2}^+$) state which was not observed by De Voigt *et al* (1971). The 6825 keV state also decays mainly to the 4431 keV state but the smaller branch of 40 ± 10% is to the 5343 keV ($\frac{9}{2}^+$) state via a 1482 keV γ ray. There was no evidence for the branches to the 3415 keV and 2234 keV states of 15 ± 10% and 25 ± 10% reported by De Voigt *et al* (1971) and we place upper limits of 5% on both possible decay modes.

The angular distribution of only the smaller branch from the 6793 keV state could be extracted from the NaI spectra as the major primary transition of 2362 keV could

not be resolved from the 2149 and 2234 keV γ rays. This angular distribution could only be fitted by spins of $\frac{5}{2}$ and $\frac{9}{2}$ ($\chi^2 = 4{\cdot}1$; $\chi^2_{0{\cdot}1\%} = 16$) both with mixing ratios close to zero; the $\frac{3}{2}$, $\frac{7}{2}$ and $\frac{11}{2}$ assignments being rejected with χ^2 values of 240, 36 and 288 respectively. The angular distribution of the 2362 keV γ ray was, however, obtained from the singles GeLi experiment and this also could only be fitted by spins of $\frac{5}{2}$ and $\frac{9}{2}$ but at mixing ratios that were both nonzero; $0{\cdot}29 \pm 0{\cdot}04$ ($\frac{9}{2}$) and $-3 < \delta < -0{\cdot}5$ ($\frac{5}{2}$). The measured lifetime of 200 ± 30 fs would yield unacceptably large M2 strengths of at least 15 Wu for both assignments indicating the parity of the state is negative. We therefore conclude that $J^\pi = \frac{5}{2}^-$ or $\frac{9}{2}^-$, which, when compared with the previous restriction of De Voigt *et al* (1971) of $J^\pi = \frac{7}{2}^-, \frac{9}{2}, \frac{11}{2}^-$ due to feeding from an $\frac{11}{2}^-$ resonance state, enables the 6793 keV state to be assigned $J^\pi = \frac{9}{2}^-$.

The 2394 keV transition from the 6825 keV state is unresolved in both the NaI spectra and the singles GeLi experiment, the latter due to the 2400 keV γ ray from the 4634 keV state. However the angular distribution of the 1482 keV primary transition was obtained from both experiments and in each case only the $\frac{7}{2}$ and $\frac{11}{2}$ spin assignments fitted the data ($\chi^2 = 8$, $\chi^2_{0{\cdot}1\%} = 16$), the $\frac{5}{2}$ and $\frac{9}{2}$ possibilities giving $\chi^2 > 67$. The measured lifetime of the state, 90 ± 30 fs, with the mixing ratio for the $\frac{7}{2}$ solution of $-0{\cdot}23 \pm 0{\cdot}06$ implies an unacceptable M2 strength of at least 120 Wu ruling out $\frac{7}{2}^-$, and the magnitude of the major 2394 keV branch to the 4431 keV ($\frac{7}{2}^-$) state enables $J^\pi = \frac{11}{2}^+$ to be ruled out due to an M2 strength of at least 350 Wu. The two remaining J^π possibilities give polarizations for the 1482 keV γ ray of $0{\cdot}04(\frac{7}{2}^+)$ and $0{\cdot}31(\frac{11}{2}^-)$ compared with the measured value of $0{\cdot}52 \pm 0{\cdot}20$. The full analysis shows the $\frac{7}{2}^+$ assignment is just excluded at the 0·2% confidence limit ($\chi^2 = 17$) compared with $\chi^2 = 10$ for the $\frac{11}{2}^-$ assignment and, therefore, we conclude the $J^\pi = \frac{11}{2}^-$ solution is very strongly favoured for the 6825 keV state.

3.16. The 6932 ($J^\pi = \frac{5}{2}^+$) and 7080 keV states

A 2649 keV γ ray observed in the singles GeLi experiment at bombarding energies of 12 and 14 MeV was assigned as a decay from the 7080 keV state to the 4431 keV ($\frac{7}{2}^-$) state.

The 6932 keV state was strongly excited in the proton–gamma coincidence experiment and decayed exclusively to the 2234 keV ($\frac{5}{2}^+$) state. The analysis of the angular distribution of the primary 4698 keV γ ray resulted in a unique $J = \frac{5}{2}$ assignment ($\chi^2 = 7{\cdot}0$, $\chi^2_{0{\cdot}1\%} = 16$, with other spin possibilities having $\chi^2 > 60$) at a mixing ratio of $1{\cdot}3 \pm 0{\cdot}3$. The previous lifetime upper limit of 40 fs (Wolff *et al* 1968) would give an M2 strength of at least 22 Wu indicating negative parity is unlikely. This confirms the previous assignment of $J^\pi = \frac{5}{2}^+$ by Wolff and Leighton (1970) from an $l_p = 2$ transfer in the ^{30}Si(^{3}He, d)^{31}P reaction.

3.17. The 7118 keV state ($J^\pi = \frac{9}{2}^+$)

The 7118 keV state, which was strongly excited in the proton–gamma coincidence experiment, decays only to the 3415 keV ($\frac{7}{2}^+$) state. The angular distributions of all three members of the cascade were fitted simultaneously resulting in the rejection of all spin possibilities ($\chi^2 > 220$) except $J = \frac{9}{2}$ ($\chi^2 = 14$, $\chi^2_{0{\cdot}1\%} = 30$) at a mixing ratio of $0{\cdot}18 \pm 0{\cdot}02$. The lifetime upper limit of 25 fs favours positive parity as the M2 strength would be at least 8 Wu.

3.18. The 7441 keV state ($J^\pi = \frac{11}{2}^+$)

The coincidence γ-ray spectrum, shown in figure 4(*c*), clearly indicates that the major 91% decay branch of the 7441 keV state is by a cascade through the 3415 keV ($\frac{7}{2}^+$) state. The coincidence GeLi spectrum confirms that there is no evidence of large branches to the 4431 keV ($\frac{7}{2}^-$) and 2234 keV ($\frac{5}{2}^+$) states of 50 ± 10% and 10 ± 5% as reported by De Voigt *et al* (1971), and we place upper limits of 5% on both these possible decay modes. However, we do propose a new 9 ± 2% branch to the 6452 keV ($\frac{11}{2}^+$) state from the observation of the 989 keV γ ray in both NaI and GeLi coincidence spectra. This weak branch was ignored in the angular distribution analysis of the 4026 and 2149 keV γ rays of the main decay mode. The resulting χ^2 plots (figure 7(*b*)) gave a unique spin assignment of $\frac{11}{2}$ at a mixing ratio of $-0{\cdot}04 \pm 0{\cdot}05$ which is consistent with pure quadrupole radiation. The measured lifetime upper limit of 15 fs gives an unacceptable M2 strength of above 250 Wu enabling the state to be assigned positive parity. The analysis of the angular distribution of the weak 989 keV γ ray from the singles GeLi experiment resulted in a rather poor limitation of its mixing ratio of $\delta = -0{\cdot}3 \pm 0{\cdot}3$.

4. Discussion

4.1. Positive parity states and the shell model

Shell-model calculations have been carried out by Wildenthal *et al* (1968) for nuclei with masses $30 \leqslant A \leqslant 33$. Particles were taken in the $2s_{1/2}$ and $1d_{3/2}$ subshells with up to two holes in the $1d_{5/2}$ subshell, and the residual interaction used was one of the surface-delta type. This enables the 63 two-body matrix elements to be specified by just four parameters which together with the three single-particle energies were determined from a least squares fit to 53 data of ground state binding energies and excitation energies in these nuclei; we denote this calculation MSDI-1. In a subsequent extension of this work (Wildenthal *et al* 1971) the MSDI parameters were established from fitting 66 data on levels in nuclei $A = 30$–34 giving slightly different parameters and wavefunctions (MSDI-2). Wildenthal *et al* (1971) also reported the results of a calculation (FPSDI) which treated the two-body matrix elements not involving the $d_{5/2}$ subshell as independent parameters. The spectra resulting from all three calculations were similar and so we have compared in table 5 the experimental level energies, where known, with the calculated energies using MSDI-2 for the lowest four levels of each spin. These show very good agreement except for the third $\frac{1}{2}^+$ state where the discrepancy is 1·28 MeV, and efforts to definitely locate a further $\frac{1}{2}^+$ state at around the calculated energy of 4 MeV have, at present, been unsuccessful. Neglecting this state the RMS deviation is 0·3 MeV. Wildenthal *et al* (1968) used the wavefunctions to calculate some single-nucleon transfer spectroscopic factors in the $^{30}Si(^3He, d)^{31}P$ reaction and obtained good agreement for those levels with $J^\pi < \frac{5}{2}^+$ on which data were available.

A further test of the MSDI wavefunctions can be obtained by calculating γ-ray transition strengths and comparing these with available data. This was first carried out by Glaudemans *et al* (1969) who calculated the log*ft* values for ^{31}S and ^{31}Si decay, and the ^{31}P magnetic moment as well as some transition strengths in ^{31}P (see table 6) using the wavefunctions from MSDI-1. They reported very good agreement with experiment for the largest M1 strengths, log *ft* values and magnetic moment, providing the isovector part of the matrix element is quenched, and for E2 strengths if the average effective charge is allowed to increase linearly with the excitation energy. However, their

Table 5. Experimental and theoretical excitation energies for ^{31}P. The theoretical energies have been calculated using the MSDI-2 parameters of Wildenthal *et al* (1971); $A_0 = 0{\cdot}646$ MeV, $A_1 = 0{\cdot}906$ MeV, $B_0 = -1{\cdot}470$ MeV, $B_1 = 0{\cdot}770$ MeV, $\epsilon(d_{3/2}) = -3{\cdot}96$ MeV, $\epsilon(s_{1/2}) = -6{\cdot}03$ MeV and $\epsilon(d_{5/2}) = -7{\cdot}56$ MeV.

	First		Second		Third		Fourth	
Spin	Experiment	Theory	Experiment	Theory	Experiment	Theory	Experiment	Theory
$\frac{1}{2}^+$	0	0	3·14	3·63	5·25	3·97	—	5·01
$\frac{3}{2}^+$	1·26	1·23	3·51	3·93	4·26	4·55	4·59	4·69
$\frac{5}{2}^+$	2·23	2·48	3·29	2·84	4·19	4·70	4·78	4·91
$\frac{7}{2}^+$	3·41	3·64	4·63	4·08	5·53	5·53	5·77	5·73
$\frac{9}{2}^+$	5·34	5·02	5·89	5·64	6·08	6·53	7·12	6·90
$\frac{11}{2}^+$	6·45	6·39	7·44	7·27	—	8·12	—	8·36
$\frac{13}{2}^+$	—	7·64	—	8·59	—	9·67	—	—

calculations did not extend to states with $J^\pi \geqslant \frac{9}{2}^+$ as no such states had, at that time, been identified. A second calculation for ^{31}P, using the wavefunctions from MSDI-2, was carried out by Glaudemans *et al* (1971) as part of a larger calculation of transition rates in $A = 30$–34 nuclei, in which effective g factors and charges were obtained from a least squares fit to data from several nuclei. The results, shown in table 6, indicate some differences with the previous calculation, notably the prediction of an even stronger E2 strength for the 3415 keV to 2234 keV transition in disagreement with the experimental data. Another calculation by Wildenthal *et al* (1971) gave transition strengths from both the MSDI-2 and FPSDI wavefunctions, using free nucleon g factors and a fixed effective charge of $0{\cdot}5e$. The resulting transition strengths, given in table 6, were generally fairly close to those predicted in the two calculations by Glaudemans *et al* indicating the three sets of wavefunctions were not vastly different. We note that the MSDI-2 calculations of Wildenthal using a fixed effective charge and bare nucleon g factors gave an overall fit that is as good as the more complicated calculations using the fitted effective charges and g factors of Glaudemans. We have therefore chosen to extend the simpler calculations to higher spin states. The wavefunctions were generated using the Glasgow–Manchester shell-model program (Whitehead 1972) with the MSDI-2 parameters, and the transition strengths, listed in table 7, were calculated assuming bare nucleon g factors, an effective charge of $0{\cdot}5e$ and taking $\hbar w = 13$ MeV.

The outstanding feature of the calculations is the large E2 strengths between the lowest states of each spin; 7·4 and 7·6 Wu from $(\frac{11}{2})^1$, 5·3 and 9·9 Wu from $(\frac{9}{2})^1$, and 2·5 and 13·1 Wu from $(\frac{7}{2})^1$. However, large E2 strengths are only observed experimentally from the $(\frac{11}{2})^1$ state with much weaker decays from the $(\frac{9}{2})^1$ state ($1{\cdot}0 \pm 0{\cdot}2$ and less than 0·9 Wu) and the stopover transition from the $(\frac{7}{2})^1$ state ($0{\cdot}8 \pm 0{\cdot}3$ Wu). The observation that the E2 strengths from the $(\frac{5}{2})^2$ and $(\frac{7}{2})^2$ states increase as the J value of the final state increases is not reproduced theoretically. Also the strongest experimental E2 decay from the $(\frac{9}{2})^1$ state is to the $(\frac{5}{2})^2$ state whilst theoretically this is essentially zero. Although this feature is present in the second theoretical $\frac{9}{2}$ state, indicating that possibly the assignment of the two $\frac{9}{2}$ states should be reversed, there would still be large discrepancies between the data and the theoretical predictions for the $(\frac{9}{2})^2 \rightarrow (\frac{5}{2})^1$ and the $(\frac{9}{2})^1 \rightarrow (\frac{7}{2})^1$ transitions. We note that, overall, the predicted and experimental M1 strengths show reasonable agreement except for the $(\frac{7}{2})^1 \rightarrow (\frac{5}{2})^1$ and $(\frac{7}{2})^2 \rightarrow (\frac{5}{2})^1$ transitions where the experimental M1 decays are very weak.

Table 6. A comparison of theoretical and experimental transition strengths for the low-lying states of ^{31}P

		M1 strength (mWu)						E2 (strength (Wu)				
Transition	Experimental	G168	G171	Wi71a	Wi71b	Ca70	Experimental	G168	G171	Wi71a	Wi71b	Ca70
1·27–0	18±4	6	15	13	12	3	3·8±1·0	4·7	5·4	4·7	4·7	2·8
2·23–0							7·3±0·7	5·1	2·2	2·1	3·6	13·5
2·23–1·27	⩽0·1	0·1	2	0·3	3		⩽0·5	1·1	0·4	0·4	0·3	
3·13–0	⩾70	110	160	250	260	102						
3·29–0							⩽0·1	1·2	2·4	1·9	1·0	
3·29–1·27	23±4	41	16	96	84	3	3·3±0·6	3·2	1·8	1·6	1·9	10·6
3·29–2·23	37±6	12	71	31	16	8	21±8	1·1	3·5	3·1	4·2	4·2
3·41–1·27							9·4±1·3	8·3	2·6	2·5	5·9	11·8
3·41–2·23	2·1±0·5	50	120	110	10	17	0·8±0·3	4·2	14	13	6·3	0·5

G168: from Glaudemans *et al* (1968) using MSDI-1 wavefunctions and energy dependent effective charges.
G171: from Glaudemans *et al* (1971) using MSDI-2 wavefunctions, effective g factors and effective charges, $e_p = 1{\cdot}44e$, $e_n = 0{\cdot}68e$.
Wi71a: from Wildenthal *et al* (1971) using MSDI-2 wavefunctions, bare nucleon g factors and effective charges, $e_p = 1{\cdot}5e$, $e_n = 0{\cdot}5e$.
Wi71b: from Wildenthal *et al* (1971) using FPSDI wavefunctions, bare nucleon g factors and effective charges, $e_p = 1{\cdot}5e$, $e_n = 0{\cdot}5e$.
Ca70: from Castel *et al* (1970), an intermediate coupling model calculation.

Table 7. A comparison of the experimental E2 and M1 transition strengths with the theoretical predictions based on the MSDI shell-model parameters

	E2 (Wu)		M1 (mWu)	
Transition	Theory	Experiment	Theory	Experiment
$(\frac{3}{2})^1 \rightarrow (\frac{1}{2})^1$	4·7	$3{\cdot}8 \pm 1{\cdot}0$	13	18 ± 4
$(\frac{5}{2})^1 \rightarrow (\frac{1}{2})^1$	2·1	$7{\cdot}3 \pm 0{\cdot}7$		
$\rightarrow (\frac{3}{2})^1$	0·4	$\leqslant 0{\cdot}5$	0·3	$\leqslant 0{\cdot}1$
$(\frac{5}{2})^2 \rightarrow (\frac{1}{2})^1$	1·9	$\leqslant 0{\cdot}1$		
$\rightarrow (\frac{3}{2})^1$	1·6	$3{\cdot}3 \pm 0{\cdot}6$	96	23 ± 4
$\rightarrow (\frac{5}{2})^1$	3·1	21 ± 8	31	37 ± 6
$(\frac{7}{2})^1 \rightarrow (\frac{3}{2})^1$	2·5	$9{\cdot}4 \pm 1{\cdot}3$		
$\rightarrow (\frac{5}{2})^1$	13·1	$0{\cdot}8 \pm 0{\cdot}3$	110	$2{\cdot}1 \pm 0{\cdot}5$
$(\frac{7}{2})^2 \rightarrow (\frac{3}{2})^1$	4·7	$0{\cdot}10 \pm 0{\cdot}03$		
$\rightarrow (\frac{5}{2})^1$	0·2	$0{\cdot}6 \pm 0{\cdot}2$	31	$4{\cdot}7 \pm 1{\cdot}3$
$\rightarrow (\frac{5}{2})^2$	2·1	15 ± 4	14	42 ± 11
$\rightarrow (\frac{7}{2})^1$	0·2	19 ± 5	67	60 ± 15
$(\frac{9}{2})^1 \rightarrow (\frac{5}{2})^1$	5·3	$1{\cdot}0 \pm 0{\cdot}2$		
$\rightarrow (\frac{5}{2})^2$	0·0	$6{\cdot}4 \pm 1{\cdot}4$		
$\rightarrow (\frac{7}{2})^1$	9·9	$\leqslant 0{\cdot}9$	140	74 ± 15
$(\frac{9}{2})^2 \rightarrow (\frac{5}{2})^1$	0·0	$6{\cdot}3 \pm 2{\cdot}0$		
$\rightarrow (\frac{5}{2})^2$	1·3	$\leqslant 1{\cdot}5$		
$\rightarrow (\frac{7}{2})^1$	0·3	$0{\cdot}2 \pm 0{\cdot}1$	16	$6{\cdot}5 \pm 2{\cdot}0$
$(\frac{11}{2})^1 \rightarrow (\frac{7}{2})^1$	7·4	15 ± 6		
$\rightarrow (\frac{9}{2})^1$	7·6	26 ± 10	200	70 ± 30
$\rightarrow (\frac{9}{2})^2$	1·3		4	
$(\frac{11}{2})^2 \rightarrow (\frac{7}{2})^1$	0·7	$\geqslant 8$		
$\rightarrow (\frac{9}{2})^1$	2·8		57	
$\rightarrow (\frac{9}{2})^2$	3·5		38	
$\rightarrow (\frac{11}{2})^1$	0·2		111	$\geqslant 180$

We conclude that the present MSDI shell-model calculations give very good agreement for excitation energies, reasonable agreement for M1 transition strengths but poor agreement overall for the E2 transition strengths.

4.2. Positive parity states and the intermediate coupling model

An intermediate coupling calculation has been reported by Castel *et al* (1970) using a ^{32}S core with hole states in the $d_{3/2}$ and $s_{1/2}$ subshells. The theoretical spectrum gives reasonable agreement for states below 4 MeV excitation energy and the transition strengths, given in table 6, are as good as those predicted by the shell-model calculations. However, the theory has limited application as it does not, at present, predict the structure of the higher spin states in ^{31}P.

4.3. Positive parity states and the Nilsson model

We now consider whether the strong coupling rotational model is useful in understanding the structure of the positive parity states in ^{31}P. Since previous attempts by Bishop *et al* (1965) and Ramavataram (1966) the amount of available experimental data has much increased and indicates that a number of the E2 transition strengths are reasonably enhanced showing that this approach may be applicable. For prolate deformation the

three lowest bands are expected to be two $K^\pi = \frac{1}{2}^+$ bands, based on the odd proton in Nilsson orbits 9 and 11 together with a $K^\pi = \frac{5}{2}^+$ hole band obtained by promoting a proton from Nilsson orbit 5 to 9. The two $K^\pi = \frac{1}{2}^+$ bands will mix and as their decoupling parameters are of opposite sign we expect some straightening of the bands. The assignments of members of the ground state $K^\pi = \frac{1}{2}^+$ and the $K^\pi = \frac{5}{2}^+$ bands up to the $\frac{7}{2}^+$ members are straightforward (figure 9), but three $\frac{9}{2}^+$ states have been identified

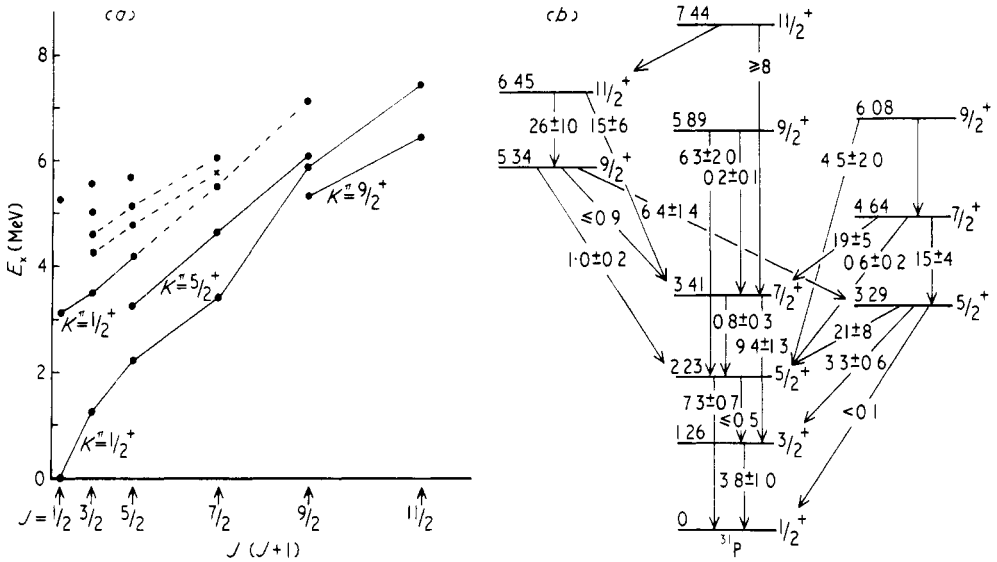

Figure 9. (*a*) A plot of excitation energy against $J(J+1)$ for the positive parity states in ^{31}P. Proposed rotational bands are labelled and broken lines indicate two further possible bands. (*b*) The E2 transition strengths in Wu that have been experimentally determined between states proposed as members of the $K^\pi = \frac{1}{2}^+$ ground state band and the $K^\pi = \frac{5}{2}^+$ and $K^\pi = \frac{9}{2}^+$ bands.

in an energy region where only two $\frac{9}{2}^+$ band members are required. The decay of the lower members of the ground state band follows the pattern expected from the simple rotational model of strong crossover ($\Delta J = 2$) and weak stopover ($\Delta J = 1$) E2 transition strengths, as shown in table 8. The only $\frac{9}{2}^+$ state that has this feature is the 5892 keV state and hence this is placed in the ground state band. An expected characteristic of the $K^\pi = \frac{5}{2}^+$ hole band is a strong stopover ($\Delta J = 1$) E2 strength and the only state that would be able to have this property is the 6078 keV state with its 12% branch to the 4634 keV ($\frac{7}{2}^+$) state although its mixing ratio and hence its transition strength have not been measured. The remaining $\frac{9}{2}^+$ state at 5343 keV has an essentially dipole transition to the 3415 keV ($\frac{7}{2}^+$) state and a fairly strong 6·4 Wu E2 decay to the 3295 keV $K^\pi = \frac{5}{2}^+$ band head. We consider that a reasonable interpretation of this state can be obtained from the rotation–vibration coupling approach as presented by Röpke *et al* (1970) for ^{25}Mg and ^{27}Al and recently extended by Price *et al* (1974). We propose that the 5343 keV state is the band head of a $K^\pi = \frac{9}{2}^+$ band based on the coupling of the $\frac{5}{2}^+$ hole state and the one-phonon core state of ^{32}S. The 2·04 MeV energy separation of the 3295 and 5343 keV states and the transition strength of 6·4 Wu are comparable with

Table 8. The E2 strengths of the crossover ($\Delta J = 2$) and stopover ($\Delta J = 1$) transitions compared with the predictions of the simple Nilsson Model. The transition strengths have been normalized using the first crossover γ ray, ie the $\frac{5}{2}^+ \rightarrow \frac{1}{2}^+$ transition

	E2 transition strengths (Wu)			
	Crossover ($\Delta J = 2$)		Stopover ($\Delta J = 1$)	
Initial spin	Experiment	Theory	Experiment	Theory
$\frac{3}{2}^+$			$3{\cdot}8 \pm 1{\cdot}0$	7·3
$\frac{5}{2}^+$	$7{\cdot}3 \pm 0{\cdot}7$	7·3	$\leqslant 0{\cdot}5$	2·1
$\frac{7}{2}^+$	$9{\cdot}4 \pm 1{\cdot}3$	9·4	$0{\cdot}8 \pm 0{\cdot}3$	1·0
$\frac{9}{2}^+$	$6{\cdot}3 \pm 2{\cdot}0$	10·4	$0{\cdot}2 \pm 0{\cdot}1$	0·6
$\frac{11}{2}^+$	$\geqslant 8$	11·1		0·4

the excitation energy of the first-excited state in ^{32}S of 2·23 MeV and its 7·3 Wu E2 strength. The 6453 keV ($\frac{11}{2}^+$) state with its strong E2 decay of 26 ± 10 Wu to the 5343 keV state is thus interpreted as the second member of this band. We note also that the sign of the mixing ratio is the same as the $\frac{7}{2}^+ \rightarrow \frac{5}{2}^+$ transition of the $K^\pi = \frac{5}{2}^+$ hole band.

The above interpretation of the positive parity states in terms of the Nilsson model, although reasonable, does not account for several strong cross-band E2 transition strengths, as illustrated in figure 9(*b*), notably the 15 ± 6 Wu (6453–3415 keV), 19 ± 5 Wu (4634–3415 keV) and 21 ± 8 Wu (3295–2234 keV) transitions. This implies considerable band mixing which, on a simple picture, should not occur directly between $K^\pi = \frac{5}{2}^+$ and $\frac{1}{2}^+$ bands. Also the out-of-band transition strengths should have roughly equal strength whereas experimentally the $\Delta J = 2$ ($\frac{5}{2}^+ \rightarrow \frac{1}{2}^+$ and $\frac{7}{2}^+ \rightarrow \frac{3}{2}^+$) are very weak, the $\Delta J = 1$ ($\frac{5}{2}^+ \rightarrow \frac{3}{2}^+$ and $\frac{7}{2}^+ \rightarrow \frac{5}{2}^+$) are stronger and the $\Delta J = 0$ ($\frac{5}{2}^+ \rightarrow \frac{5}{2}^+$ and $\frac{7}{2}^+ \rightarrow \frac{7}{2}^+$) are very strong.

4.4. Negative parity states

The present work has established the existence of two $\frac{9}{2}^-$ states at 6500 and 6793 keV and one $\frac{11}{2}^-$ state at 6825 keV. Lower spin negative parity states had previously been identified by Wolff and Leighton (1970) from the ^{30}Si(^{3}He, d)^{31}P reaction and the excitation energies of all these states are illustrated in figure 10. The most striking feature is the concentration of states around 6·7 MeV approximately 2 MeV above the mainly single-particle $\frac{3}{2}^-$ and $\frac{7}{2}^-$ states at 4431 and 5015 keV. This strongly suggests that vibrational features are playing a dominant role. The simple coupling of the $\frac{3}{2}^-$ and $\frac{7}{2}^-$ particles to a single-phonon core yields sets of states from $\frac{1}{2}^-$ to $\frac{7}{2}^-$ and $\frac{3}{2}^-$ to $\frac{11}{2}^-$ respectively. Hence experimentally one $\frac{7}{2}^-$ state is missing and there is an extra $\frac{9}{2}^-$ state. As the only information on transition strengths is the present data on states with $J^\pi \geqslant \frac{7}{2}^-$ the model cannot really be fully tested. However two of these states, at 6500 ($\frac{9}{2}^-$) and 6825 keV ($\frac{11}{2}^-$), have strong E2 strengths of 31 ± 11 and 12 ± 4 Wu to the 4431 keV ($\frac{7}{2}^-$) state, and the latter state also has an unusually strong $1{\cdot}4 \pm 0{\cdot}4$ mWu E1 transition to the 5343 keV ($\frac{9}{2}^+$) state, which has already been interpreted as a particle–core coupled state. We note, however, that the other two states have only weak E2 strengths of less than 1·7 and $0{\cdot}5 \pm 0{\cdot}1$ Wu to the 4431 keV ($\frac{7}{2}^-$) state, in disagreement with the behaviour expected from the above interpretation.

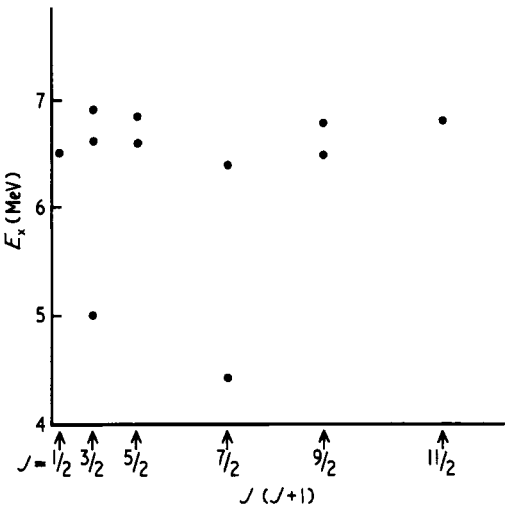

Figure 10. A plot of excitation energy against $J(J+1)$ for the negative parity states in ^{31}P.

5. Conclusion

Experimental results have been presented that have enabled J^π values to be assigned, branching ratios, multipole mixing ratios and mean lifetimes to be determined for many states in ^{31}P. These include a number of higher spin positive parity states which has led to possible interpretation of their structure based on the Nilsson model with rotation–vibration coupling. Also the shell-model calculations using the MSDI interaction have been extended to include the transition strengths from higher spin positive parity states which give rather poor agreement with the new data.

Acknowledgments

We wish to thank Mr V Pucknall for invaluable assistance with the shell-model calculations and the Science Research Council for their financial support of the experimental programme and for a studentship held by PRGL. One of us (EMJ) wishes to thank the University of Ceylon for financial assistance. We thank Mr J Reynolds for the preparation of the targets and Mr M Patterson for manufacturing the surface barrier detectors.

References

Bishop G R, Bottino A and Lombard R M 1965 *Phys. Lett.* **15** 323–4
Blaugrund A E 1966 *Nucl. Phys.* **88** 501–12
Butler P A *et al* 1973 *Nucl. Instrum. Meth.* **108** 497–502
Castel B, Stewart K W C and Harvey M 1970 *Can. J. Phys.* **48** 1490–8
Cujec B *et al* 1965 *Phys. Lett.* **15** 266–8
De Voigt M J A, Regenboog D A, Grootenhuis J and van der Leun C 1971 *Nucl. Phys.* A **176** 97–109
Endt P M and van der Leun C 1973 *Nucl. Phys.* A **214** 1–625

Glaudemans P W M, Dieperink A E L, Keddy R J and Endt P M 1969 *Phys. Lett.* **28B** 645–7
Glaudemans P W M, Endt P M and Dieperink A E L 1971 *Ann. Phys., NY* **63** 134–70
Harris G I and Breitenbecher D V 1966 *Phys. Rev.* **145** 866–87
James A N, Twin P J and Butler P A 1974 *Nucl. Instrum. Meth.* **115** 105–13
Moss C E 1969 *Nucl. Phys.* A **124** 440–4
Price H G *et al* 1974 *J. Phys.* A: *Math., Nucl. Gen.* **7** 1151–5
Ramavataram K 1966 *Phys. Lett.* **21** 690–2
Röpke H, Glattes V and Hammel G 1970 *Nucl. Phys.* A **156** 477–88
Rose H J and Brink D M 1967 *Rev. Mod. Phys.* **39** 306–47
Sharpey-Schafer J F *et al* 1971 *Nucl. Phys.* A **167** 602–24
Scott H L and van Patter D M 1969 *Phys. Rev.* **184** 1111–6
Sheldon E and van Patter D M 1966 *Rev. Mod. Phys.* **38** 143–86
Van Rinsvelt H A and Endt P M 1966 *Physica* **32** 529–47
Whitehead R R 1972 *Nucl. Phys.* A **182** 290–300
Wildenthal B H, McGrory J B, Halbert E C and Glaudemans P W M 1968 *Phys. Lett.* **27B** 611–3
Wildenthal B H, McGrory J B, Halbert E C and Graber H D 1971 *Phys. Rev.* C **4** 1708–58
Willmes H and Harris G I 1967 *Phys. Rev.* **162** 1027–35
Wolff A C, Boelhouwer W C R and Endt P M 1969 *Nucl. Phys.* A **124** 273–86
Wolff A C and Leighton H G 1970 *Nucl. Phys.* A **140** 319–22
Wolff A C, Mayer M A and Endt P M 1968 *Nucl. Phys.* A **107** 332–46